Earth Surf. Dynam. Discuss., https://doi.org/10.5194/esurf-2018-83
Manuscript under review for journal Earth Surf. Dynam.
Discussion started: 3 December 2018

Earth Surface Dynamics Discussions
Open Access
EGU

Cosmogenic ^{10}Be in river sediment: where grain size matters and why

Renee van Dongen[1], Dirk Scherler[1,2], Hella Wittmann[1] and Friedhelm von Blanckenburg[1,2]

[1]GFZ German Research Centre for Geosciences, Earth Surface Geochemistry, Telegrafenberg, 14473 Potsdam, Germany.
[2]Freie Universität Berlin, Institute for Geological Sciences, 12249 Berlin, Germany.

Correspondence to: Renee van Dongen (dongen@gfz-potsdam.de)

Earth Surf. Dynam. Discuss., https://doi.org/10.5194/esurf-2018-83
Manuscript under review for journal Earth Surf. Dynam.
Discussion started: 3 December 2018

Abstract

Concentrations of *in situ*-produced cosmogenic ^{10}Be in river sediment are widely used to estimate catchment-average denudation rates. Typically, the ^{10}Be concentrations are measured in the sand fraction of river sediment. However, the grain size of bedload sediment in most bedrock rivers cover a much wider range. Where ^{10}Be concentrations depend on grain size, denudation rate estimates based on the sand fraction alone could potentially be biased. To date, knowledge about catchment attributes that may induce grain size-dependent ^{10}Be concentrations is incomplete or has only been investigated in modelling studies. Here we present an empirical study on the occurrence of grain size-dependent ^{10}Be concentrations and the potential controls of hillslope angle, precipitation, lithology and abrasion. We first conducted a study focusing on the sole effect of precipitation in four granitic catchments located on a climate-gradient in the Chilean Coastal Cordillera. We found that observed grain size dependencies of ^{10}Be concentrations in the most-arid and most-humid catchments could be explained by the effect of precipitation on both the scouring depth of erosion processes and the depth of the mixed soil layer. Analysis of a global dataset of published ^{10}Be concentrations in different grain sizes (n=62 catchments), comprising catchments with contrasting hillslope angles, climate, lithology and catchment size revealed a similar pattern. Lower ^{10}Be concentrations in coarse grains (defined as "negative grain size dependency") emerge frequently in catchments which likely have thin soil and where deep-seated erosion processes (e.g. landslides) excavate grains over a larger depth-interval. These catchments include steep (>25°), arid (<100 mm yr^{-1}) and humid catchments (>2000 mm yr^{-1}). Furthermore, we found that an additional cause of negative grain size dependencies may emerge in large catchments with long sediment travel distances (>2300-7000 m, depending on lithology) where abrasion and sediment provenance may lead to a grain size distribution that is not representative for the entire catchment. The results of this study can be used to evaluate whether catchment-average denudation rates are likely to be biased in particular catchments.

Earth Surf. Dynam. Discuss., https://doi.org/10.5194/esurf-2018-83
Manuscript under review for journal Earth Surf. Dynam.
Discussion started: 3 December 2018

1. Introduction

Catchment-average denudation rates are commonly estimated with *in situ*-produced cosmogenic ^{10}Be concentrations in river sediment (Bierman and Steig, 1996; von Blanckenburg, 2005; Granger et al., 1996). ^{10}Be is a rare isotope that is produced within quartz minerals by high-energy cosmic rays in the upper few meters of the Earth's surface (Gosse and Phillips, 2003). Its concentration records the time minerals were exposed to cosmic radiation, which is inversely proportional to denudation rates over time scales of 10^2-10^5 years (Lal, 1991). Most studies use a sand fraction (0.1-2 mm) of river bedload sediment to estimate catchment-average denudation rates. However, bedload grain sizes found in bedrock rivers, where this method is frequently applied, are often much coarser (Figure 1). The sand fraction provides a representative catchment-average denudation rate only if it is spatially and temporally representative for all erosion sources within the catchment (Bierman and Steig, 1996; von Blanckenburg, 2005; Gonzalez et al., 2017; Granger et al., 1996; Neilson et al., 2017; Willenbring et al., 2013). Evaluating this condition is challenging and requires a detailed understanding of the catchment and its erosion processes. Where ^{10}Be concentrations differ amongst grain size fractions, using a non-representative grain size fraction could result in biased catchment-average denudation rates.

To date, there is no general consensus of what causes grain size-dependent ^{10}Be concentrations in a catchment. Some studies inferred that lower ^{10}Be concentrations in coarse grains are caused by deep-seated erosion processes, such as landslides, which excavate material from greater depth where ^{10}Be concentrations are lower (Aguilar et al., 2014; Belmont et al., 2007; Brown et al., 1995; Puchol et al., 2014; Schildgen et al., 2016; Tofelde et al., 2018; West et al., 2014). In a recent study Tofelde et al. (2018) combined a detailed inventory of hillslope processes in a large, semi-arid Andean catchment, with ^{10}Be concentrations measured in the sand and gravel fraction of river sediment. They explained lower ^{10}Be concentrations in the gravel compared to the sand by the scouring depth of erosion processes. However, other studies found that grain size reduction by abrasion during fluvial transport, or spatial variations in the provenance of different grains sizes can additionally account for grain size-dependent ^{10}Be concentrations. This is particularly true for large and high-relief catchments that cover large elevation ranges, because ^{10}Be production rates depend on atmospheric depth (Carretier et al., 2009; Carretier and Regard, 2011; Lukens et al., 2016; Lupker et al., 2017; Matmon et al., 2003). Carretier et al. (2015) conducted a comprehensive study on ^{10}Be concentrations in different grain sizes on a climate gradient, sampling large Andean catchments. Despite significant contrasts in precipitation and, presumably, weathering and erosion processes, no systematic grain size dependency of ^{10}Be concentrations as result of precipitation emerged. A reason may be that as catchment size increases, more complexity in controlling factors is added that may blur potential trends in the data. Hence, it remains elusive which type of catchments are sensitive to grain size-dependent ^{10}Be concentrations and biased catchment-average denudation rates (e.g., Carretier et al., 2015), or it has only been addressed in modelling studies (e.g. Lukens et al., 2016).

This paper presents the results of an empirical study in which we investigated the occurrence and cause of grain size-dependent ^{10}Be concentrations in river sediment. Our study consists of two parts: in the first part, we investigated the sole effect of precipitation, in small, granitic catchments in the Chilean Coastal Cordillera that differ mainly by mean annual precipitation. In the second part, we compiled and investigated a global dataset with previously published grain size-dependent ^{10}Be concentrations to include more catchment attributes in our analysis. In the following, we first

provide a review of processes that control the grain size distribution and ^{10}Be concentrations of river sediment, to determine relevant catchment attributes for our analysis.

2. Why ^{10}Be concentrations in river sediment can depend on grain size

2.1 Processes that control grain size

The grain size distribution of river sediment is a function of (1) host rock lithology, (2) erosion and weathering processes that reduce grain size, (3) sorting on hillslopes, and (4) hydrodynamic sorting, mixing and abrasion during fluvial transport. Chemical weathering converts bedrock into sediment at a rate that is controlled by the mineralogy, lithology, and fracture spacing of the host rock, water flow, and denudation rate at the surface. The mineralogy sets dissolution rates and constrains the minimum size of individual minerals (Sklar et al., 2017). Bedrock fractures provide water pathways and expose fresh bedrock to weathering (Lebedeva and Brantley, 2017; Oberlander, 1972; Ruxton and Berry, 1957). As chemical weathering is set by the flux and temperature of water flowing through the regolith, there is also a strong dependency on the climatic regime (Lasaga et al., 1994; Maher, 2010). The size reduction of bedrock fragments in the regolith depends, besides the chemical weathering rate, also on the time they spend in the regolith layer. This regolith residence time is controlled by the thickness of the regolith layer and the denudation rate, i.e., the rate of sediment removal from the surface (Anderson et al., 2007; Attal et al., 2014; Sklar et al., 2017).

Hillslope sediment is transported towards river channels by a variety of erosion processes. Diffusive processes are considered to operate in slowly eroding landscapes and move relatively fine grains at or near the surface (Roering et al., 1999). In contrast, deep-seated erosion processes (e.g., landslides) are frequent in rapidly-eroding landscapes and excavate sediment and bedrock fragments of any size, also from greater depth (Casagli et al., 2003).

Once the sediment has been transported to the channel, processes like downstream abrasion and hydrodynamic sorting influence the grain size distribution, resulting in progressively smaller grains. Downstream abrasion wears off the outer layers of a grain (Kodoma, 1994; Sklar et al., 2006), whereas hydrodynamic sorting preferentially deposits coarse grains when the transport capacity of the water is too low (Ferguson et al., 1996; Hoey and Ferguson, 1994). Grain size reduction by abrasion is thought to depend on the travel distance and velocity as well as the lithology of the grains (Attal and Lavé, 2009). In summary, lithology, climate and the magnitude of denudation rates ought to control the grain size distribution of rock fragments on hillslopes, whereas abrasion and hydrodynamic sorting influence the grain size distribution during fluvial transport.

2.2 Processes that control ^{10}Be concentrations

^{10}Be concentrations in quartz grains depend on the ^{10}Be production rate and a grains' exposure time to cosmic rays (Gosse and Phillips, 2001). Any process that transports different grain sizes, from areas in a catchment with contrasting ^{10}Be production rates or exposure times (i.e., denudation rates), could result in ^{10}Be concentrations that differ between grain sizes. Because ^{10}Be production rates decrease exponentially with depth (Gosse and Phillips, 2001), hillslope sediment that is excavated over a larger depth interval by landslides will obtain a larger variation in ^{10}Be concentrations than sediment transported by diffusive processes near the surface (Aguilar et al., 2014; Belmont et al., 2007; Brown

et al., 1995; Puchol et al., 2014; Tofelde et al., 2018; West et al., 2014). In soil-mantled landscapes, bioturbation by burrowing animals and tree throw (Gabet et al., 2003) results in a well-mixed surface layer with a uniform ^{10}Be concentration (Brown et al., 1995; Granger et al., 1996; Schaller et al., 2018) (Figure 2). These mixed soil layers are most likely to develop in humid and slowly eroding catchments, where biota is abundant. Sediment eroded from these layers is thus expected to have uniform ^{10}Be concentrations. In rapidly eroding and arid landscapes, however, soils are typically very thin or absent, and the eroded sediments likely yield larger variations in ^{10}Be concentrations (Figure 2). Furthermore, fluvial processes can affect grain size fractions in a way that not all parts of a catchment are equally represented at a given sample location. Combined with elevation-dependent ^{10}Be production rates (and provided that denudation rates are constant), this could result in grain size-dependent ^{10}Be concentrations (Carretier et al., 2015; Lukens et al., 2016; Matmon et al., 2003). For example, sediment provenance of different grain sizes from different elevations could play a role in catchments with heterogeneous rock types or heterogeneities in quartz abundance and grain size (Bierman and Steig, 1996; Carretier et al., 2015). An unequal representation of elevations in different grain size fractions may also result from hydrodynamic sorting, downstream abrasion during fluvial transport, and insufficient mixing of tributaries that drain different elevations (Carretier et al., 2009; Carretier and Regard, 2011; Lukens et al., 2016; Neilson et al., 2017).

To summarise, grain size-dependent ^{10}Be concentrations may emerge in catchments where soil mixing by biota is absent and deep-seated erosion processes transport grains from greater depth and in catchments, where large gradients in ^{10}Be production rates combine with processes like sorting, abrasion and insufficient mixing.

Due to their effect on grain size distribution and grain size-dependent ^{10}Be concentrations, we will focus on the catchment attributes mean basin slope, mean travel distance, mean annual precipitation (MAP), and lithology. Here, we consider mean basin slope as a catchment attribute to represent denudation process, and mean travel distance to be a metric for abrasion and hydrodynamic sorting during fluvial transport.

3. Study area

For our case study, we selected 4 small catchments (<10 km^2) located in the Coastal Cordillera of central Chile (Table 1, Figure 3). The Coastal Cordillera features a pronounced latitudinal climate and vegetation gradient, whereas the tectonic setting is rather uniform. The selected catchments are located in the National Park Pan de Azúcar (AZ) (~26° S), the National Reserve Santa Gracia (SG) (~30° S), the National Park La Campana (LC) (~33° S) and the National Park Nahuelbuta (NA) (~38° S). The catchments share a granodioritic lithology, though some variations in mineralogy exist (Oeser et al., 2018). The three northern catchments experience modern uplift rates of <0.1 mm yr^{-1} (Melnick, 2016). The southern-most catchment is located in the Nahuelbuta Range, where uplift rates increased from 0.03-0.04 mm yr^{-1} to >0.2 mm yr^{-1} at 4 ± 1.2 Ma (Glodny et al., 2008; Melnick et al., 2009). Because the sampled catchment is located upstream of a river channel knickpoint, it may not yet be influenced by the increased uplift rates (Crosby and Whipple, 2006). The climatic regime and mean annual precipitation (MAP) vary from arid (MAP ~13 mm yr^{-1}) in Pan de Azúcar in the north, to semi-arid in Santa Gracia (MAP ~88 mm yr^{-1}), Mediterranean in La Campana (MAP ~358 mm yr^{-1}), and temperate in Nahuelbuta (MAP ~1213 mm yr^{-1}) in the south (Meyer-Christoffer et al., 2015). This latitudinal increase in MAP results in an increase in vegetation density. The Normalized Difference Vegetation Index

(NDVI) (Didan, 2015) varies from 0.1 in the northern-most catchment to 0.8 in the southern-most catchment (Figure S1). The increase in MAP also revealed an increase of chemical weathering rates and soil mixing depths measured in 4 soil profiles within the catchments. The chemical depletion fraction (CDF), a measure to quantify chemical weathering (Riebe et al., 2003), increases from ~0.1 in Pan de Azúcar (AZ), to ~0.4-0.5 in Santa Gracia (SG), and ~0.3-0.6 in La Campana (LC). Due to heterogeneities in bedrock samples collected in Nahuelbuta (NA), no reliable CDF could be assigned (Oeser et al., 2018). The depth of the mixed soil layer increases from ~0-17.5 cm in Pan de Azúcar (AZ), to ~25-45 cm in Santa Gracia (SG), ~47.5-85 cm in La Campana and ~70 cm in Nahuelbuta (NA) (Schaller et al., 2018). The Chilean Coastal Cordillera therefore provides a natural laboratory that allows us to explore the relationship between grain size and ^{10}Be concentrations as controlled by precipitation.

4. Methods

4.1 Sampling and analytical methods

In each of the four Chilean catchments, we collected approximately 6 kg sand and pebbles from the active channel (Figure 3) and conducted a Wolman pebble count (Wolman, 1954) with 1 m intervals to measure the grain size distribution at the sample locations (Figure S2). We dried and sieved the samples in the laboratory to separate the grain size fractions 0.5-1 mm, 1-2 mm, 2-4 mm, 4-8 mm, 8-16 mm, 16-32 mm and 32-64 mm. Before further processing, we crushed pebbles larger than 1 mm. To isolate pure quartz, we separated and purified the river sediment using standard physical and chemical separation methods (Kohl and Nishiizumi, 1992). We spiked between 10 to 20 g of pure quartz with 0.15 mg ^{9}Be carrier, dissolved the quartz and extracted beryllium following established protocols (e.g. von Blanckenburg et al., 2004). Accelerator mass spectrometry measurements were carried out at the University of Cologne, Germany. Reported ^{10}Be/^{9}Be ratios have been normalized to the KN01-6-2 and KN01-5-3 standards, with nominal ^{10}Be/^{9}Be ratios of 5.35×10^{-13} and 6.32×10^{-12}, respectively. We calculated ^{10}Be concentrations from ^{10}Be/^{9}Be ratios and a blank correction was performed. We used MATLAB® and the CRONUS functions (Balco et al., 2008) with the Lal-Stone (St) time-independent scaling scheme (Lal, 1991; Stone, 2000) and the SLHL production rate of 4.01 at g^{-1} yr^{-1} as summarized by Phillips et al. (2016) to calculate catchment-average denudation rates from the ^{10}Be concentrations

4.2 Global compilation

We compiled data from previously published studies that measured ^{10}Be concentrations in different grain size fractions sampled at the same location. Because we are interested in small to medium-sized bedrock catchments, and in order to be independent of the effect of long-term floodplain sediment storage in large basins, we discarded basins with an area of >5000 km^2. As the weathering and erosion processes affecting two sand-sized grain size fractions may be too similar, we only selected studies measuring at least one or more sand fractions (mean grain size <2 mm) and one or more coarser grain size fractions (mean grain size >2 mm) (Aguilar et al., 2014; Belmont et al., 2007; Brown et al., 1995; Carretier et al., 2015; Clapp et al., 2002; Derrieux et al., 2014; Heimsath et al., 2009; Matmon et al., 2003; Palumbo et al., 2011; Puchol et al., 2014; Reinhardt et al., 2007; Stock et al., 2009; Sullivan, 2007). From each selected

catchment we compiled the reported grain size classes, the corresponding ^{10}Be concentrations (±2σ), and the sample location coordinates (Table S3). For studies that reported a grain size fraction as 'larger than', we assumed that the upper grain size limit corresponds to twice the lower limit (e.g. reported: >2 mm, data compilation: 2-4 mm). We acknowledge that this range might be incorrect, but a fixed grain size range was required for proper data analysis.

To compare data from different study areas and from studies that measured different grain size classes, we normalized the ^{10}Be concentrations (±2σ) and grain size classes by the arithmetic mean concentration and grain size class of all samples from the same catchment. This allows us to compare the slope of the trend between finer and coarser grains, independent of the actual grain size fractions that were measured in the original studies. However, we acknowledge that we may lose information about potential breaks in trends that are related to specific grain sizes.

Based on our discussion of processes that influence the grain size distribution and ^{10}Be concentrations of river sediment (paragraph 2), we decided to focus on the following catchment attributes: mean basin slope, mean travel distance, mean annual precipitation, and lithology in our further analysis. Here, we consider mean basin slope as a catchment attribute to represent denudation rate, and mean travel distance to be a metric for abrasion and hydrodynamic sorting during fluvial transport.

We used a 90-m resolution SRTM DEM (Jarvis et al., 2008) to recalculate published sample characteristics like catchment area, mean basin slope, total relief (maximum elevation - minimum elevation) and the mean travel distance of grains to the sample location (arithmetic mean of travel distances calculated between each pixel in the catchment and the sampling point). The agreement between the published and recalculated values is good, and minor deviations likely result from differences in DEM resolution (Figure S3). We obtained an estimate of mean annual precipitation (MAP) in each catchment using the 0.25°-resolution gridded precipitation data set from the Global Precipitation Climatology Centre (GPCC; Meyer-Christoffer et al., 2015). To determine catchment lithology we used the Global Lithological Map (GLiM; Hartmann & Moosdorf, 2012) in combination with the lithology reported in the original publications. We defined four different lithological classes: sedimentary, magmatic, metamorphic and mixed (>3 different lithologies in a catchment).

We used Sternberg's Law to estimate the extent of abrasion of bedload sediment during fluvial transport as a function of travel distance *L*:

$$D(L) = D_0\, e^{-\alpha L} \quad (1)$$

Using equation 1, we calculated the grain size *D* at the sample location, which remains from an initial grain size D_0 at the source, that travelled a distance *L* and decreased in size according to the reduction coefficient α (Kodama, 1994; Kodoma, 1994; Lewin and Brewer, 2002; Sklar et al., 2006; Sklar and Dietrich, 2008). The reduction coefficient depends on both grain velocity and lithology. Rocks with low tensile strength decrease faster in size during transport compared to rocks with high tensile strength (Attal and Lavé, 2009). We chose the reduction coefficients based on literature values for different field settings (sedimentary rocks: α = 0.0003 m^{-1}, magmatic rocks: α = 0.0002 m^{-1}, metamorphic rocks: α = 0.0001 m^{-1}), which are typically higher than experimental studies due to different particle collision dynamics and the lack of weathering in experimental studies (Sklar et al., 2006). We defined an abrasion threshold for each lithology, which is based on the travel distance, at which abrasion starts to become significant. We defined the effect of abrasion to be negligible when a grain size at the erosion source (D_0) still falls in the same

Wentworth grain size class at the sample location (D). For abrasion to be significant, a grain size of 2 mm at the erosion source, for example, must be reduced by more than 50%, hence be smaller than 1 mm at the sample location. This results in abrasion thresholds for sedimentary, magmatic, and metamorphic rocks of 2300 m, 3500 m, and 7000 m, respectively. For catchments underlain by mixed lithologies, the abrasion threshold lies between 2300 m and 7000 m (Attal and Lavé, 2009). We quantified the relationship between grain size and ^{10}Be concentration by calculating a 'grain size dependency' for each sample set, which corresponds to the regression coefficient of a linear model fitted to all samples within a sample set. A positive grain size dependency indicates higher ^{10}Be concentrations in coarser grains, and vice versa. To account for uncertainties in ^{10}Be concentrations and for grain size ranges, we used a Monte Carlo approach (n=10,000) to randomly select a point between the mean ± 2σ ^{10}Be concentrations and the analysed grain size range. We thus obtained a mean ± 2σ grain size dependency for each catchment. Next, we calculated the statistics of a linear regression between the grain size dependency and one or more of the catchment attributes. We did this for the entire dataset and for each individual lithology. Finally, we calculated the relative importance (RI) of mean basin slope, mean travel distance and MAP, which is the percentage of contribution to the multivariate regression model R^2. We used the LMG approach (Lindeman, Merenda and Gold, 1980), which is part of the 'Relaimpo' R studio-package (Grömping, 2006).

5. Results

5.1 Chilean Coastal Cordillera

The measured ^{10}Be concentrations in the most arid catchment (AZ) range from 2.8 to 4.6 $\times10^5$ atoms (g quartz)$^{-1}$, resulting in catchment-average denudation rates of 5.8 ± 0.7 to 10.1 ± 1.1 mm kyr^{-1} (Table 2, Figure 4). In the semi-arid catchment (SG), the ^{10}Be concentrations range from 3.6 to 5.2 $\times10^5$ atoms (g quartz)$^{-1}$, which corresponds to catchment-average denudation rates of 7.5 ± 0.8 to 11.0 ± 1.4 mm kyr^{-1} (Table 2, Figure 4). The ^{10}Be concentrations in the Mediterranean catchment (LC) are a factor 10 lower compared to the other catchments and range from 0.2 to 0.6 $\times10^5$ atoms (g quartz)$^{-1}$, which results in catchment-average denudation rates of 103.7 ± 12.4 to 384.1 ± 54.5 mm kyr^{-1} (Table 2, Figure 4). The temperate catchment (NA) yielded ^{10}Be concentrations ranging from 1.8 to 2.9 $\times10^5$ atoms (g quartz)$^{-1}$, resulting in catchment-average denudation rates of 24.0 ± 2.6 to 40.2 ± 4.5 mm kyr^{-1} (Table 2, Figure 4). Only the arid (AZ) and Mediterranean (LC) catchments show a consistent trend between ^{10}Be concentrations and grain sizes. In the arid catchment (AZ), ^{10}Be concentrations are decreasing with increasing grain size, with a 2σ-deviation of ~18% from the mean. In the Mediterranean catchment (LC), ^{10}Be concentrations deviate up to ~40% from the mean and display a noisy but positive grain size dependency, i.e., they increase with grain size. In both the semi-arid (SG) and temperate catchments (NA), the 2σ-deviations between ^{10}Be concentrations are low (~12% and ~14%, respectively) and rather unsystematic. The smallest grain size fractions (0.5-4 mm) in the semi-arid catchment (SG) show a decreasing trend, but this trend increases again for coarser grain size fractions (4-32 mm). In the temperate catchment (NA), the ^{10}Be concentration are uniform in the five smallest grain size fractions (0.5-16 mm), but this trend breaks down at the two largest grain size fractions (16-64 mm), which have lower ^{10}Be concentrations.

Earth Surf. Dynam. Discuss., https://doi.org/10.5194/esurf-2018-83
Manuscript under review for journal Earth Surf. Dynam.
Discussion started: 3 December 2018

5.2 Global compilation

The global compilation includes 62 catchments covering a wide range of hillslope angles, sediment travel distances and MAP (Figure 5). Figure 6 shows normalized ^{10}Be concentrations and grain sizes of all catchments, for different classes of mean hillslope angle, and colour-coded by mean annual precipitation. Uncertainties in ^{10}Be concentrations tend to be higher for samples from steeper hillslope angles (>10°), which is related to generally lower concentrations, i.e., higher denudation rates. In catchments with mean basin hillslope angles <10°, ^{10}Be concentrations are nearly similar across all grain size classes, whereas catchments with hillslope angles >25° reveal distinctly lower ^{10}Be concentrations in coarse compared to fine grains (Figure 6). We discern no obvious pattern related to mean annual precipitation.

Figure 7 shows the grain size dependencies for all catchments, resulting from the regression coefficient of a fitted linear model to the normalized data from each catchment. Overall, we observe more sample sets that display significantly negative (54.8%) trends in grain size-dependent ^{10}Be concentrations than positive (25.8%; Figure 7). 19.4% of the sample sets have grain size dependencies that are not significantly different from zero, i.e., no trend. Furthermore, positive trends are typically weaker (lower absolute grain size dependencies) than negative trends.

The calculated grain size dependencies of individual catchments reveal a breakpoint at a mean hillslope angle of ~15° (Figure 7a). Catchments with mean hillslope angles <15° reveal weak grain size dependencies. The scatter and amount of negative grain size dependencies (i.e., lower ^{10}Be concentrations in coarse grains) increase at mean hillslope angles >15°, with the most negative grain size dependencies in catchments of >25°. Our analysis of sediment travel distance shows that negative grain size dependencies predominantly occur at longer sediment travel distances, when abrasion thresholds are exceeded (Figure 7b). Finally, the highest number of negative grain size dependencies are found for very dry (<100 mm yr^{-1}) and very wet catchments (>2000 mm yr^{-1}) (Figure 7c). When differentiating the catchments by lithology, the influences of hillslope angle, travel distance, and MAP are partly accentuated and partly muted. Catchments underlain by mixed lithologies (75.0%) show the largest number of negative grain size dependencies, followed by catchments underlain by sedimentary and metamorphic rocks (both 60.0%). The number of significant negative grain size dependencies is lowest for catchments underlain by magmatic lithologies (26.7%).

When considering the combined influence of all studied factors (i.e., slope, travel distance and MAP) with a multivariate linear model, we found that most of the variance of catchments with mixed lithology is explained by travel distance (RI = 25.0% ± 4.7%) and MAP (RI = 17.5% ± 4.7%) (Table S5, Figure 9). In magmatic catchments, a large proportion of the variance is explained by MAP (RI= 43.8% ± 13.1%). This trend, however, mainly results from two negative data points at higher MAP. The RI statistics yielded low values for the other lithologies, possibly, due to too few catchments to disclose unambiguous trends.

6. Discussion

6.1 Grain size-dependent ^{10}Be concentrations in the Chilean Coastal Cordillera

The sampled catchments on a climatic gradient in the Chilean Coastal Cordillera show only minor variations in ^{10}Be concentrations, regardless of grain size. Only in the arid (AZ) and Mediterranean (LC) catchments, trends in ^{10}Be

Earth Surf. Dynam. Discuss., https://doi.org/10.5194/esurf-2018-83
Manuscript under review for journal Earth Surf. Dynam.
Discussion started: 3 December 2018

concentrations with grain size exist. In both catchments, the ^{10}Be concentrations of river sediment correspond to concentrations measured deeper within soil profiles (Figure 8; Schaller et al., 2018). In the arid catchment (AZ), both the negative grain size dependencies and the fact that ^{10}Be concentrations correspond to concentrations deeper in the soil profiles suggest that deep-seated erosion processes (e.g. landslides, debris flows), which excavate sediment from greater depth during rare precipitation events, may occur in this catchment. In fact, landslides triggered by heavy precipitation events linked to El-Niño have been reported in the Atacama desert (Mather et al., 2014; Pinto et al., 2008). The noisy, but overall positive, grain size dependency in the Mediterranean catchment (LC) contradicts with observed evidence of debris flows in this catchment (Figure S5), as these would presumably also excavate material from greater depth. Furthermore, higher ^{10}Be production rates at the elevation where debris flows originate, cannot account for the positive grain size dependency alone Figure S5). It is also notable that all of the measured river sediment concentrations are considerably lower than those measured in the mixed soil layer of two soil profiles within the catchment. Without being able to clarify this issue, the lower ^{10}Be concentrations of river sediment, combined with the observed greater scatter in the positive grain size dependency may hint at selective transport and longer residence times of coarse grains at higher elevations. In contrast, the ^{10}Be concentrations in river sediments from the semi-arid (SG) and temperate (NA) catchments show little variations and are similar to concentrations measured near the surface in soil pits (Schaller et al., 2018). Within the temperate catchment (NA), the uniform ^{10}Be concentrations in grains <16 mm, suggests that these originate from the ~70 cm thick mixed soil layer, whereas the lower ^{10}Be concentrations in grains >16 mm suggests these may be derived from below the mixed layer (Figure 8). In the semi-arid (SG) catchment, the measured samples from the channel show similar ^{10}Be concentrations compared to those measured in the mixed soil layer of the north-facing hillslope and higher ^{10}Be concentrations compared to the mixed layer of the south-facing hillslope (Figure 8; Schaller et al., 2018). This suggests that grains are unlikely to be derived from greater depth, where ^{10}Be concentrations are lower.

In summary, our new samples from the Chilean Coastal Cordillera demonstrate minor variations in ^{10}Be concentrations. The influence of MAP on grain size-dependent ^{10}Be concentrations in the most-arid and most-humid catchments may reflect the thickness of the mixed soil layer and the scouring depth of erosion processes that transport larger grains from below the mixed soil layer.

6.2 Grain size-dependent ^{10}Be concentrations in the global compilation

6.2.1 Mean basin slope

The effect of mean basin slope on grain size-dependent ^{10}Be concentrations is apparent as weak grain size dependencies in gently sloping catchments, and predominantly negative grain size trends in steep catchments (Figure 6, Figure 7a). Mean basin slope may also control grain size-dependent ^{10}Be concentrations through its effect on the thickness of soils and the scouring depth of erosion processes.

In gently-sloping catchments, denudation rates are typically low (e.g., Portenga and Bierman, 2011) and well-mixed soil layers with uniform ^{10}Be concentrations can develop. Diffusive erosion processes transport sediment at and near the surface. In contrast, in steep landscapes, denudation rates are typically high, soils are thin or absent if denudation rates exceed the soil production limit (~170 mm kyr^{-1}; Dixon and von Blanckenburg, 2012). Such catchments are

typically dominated by deep-seated hillslope processes (Hovius et al., 1997). Negative grain size dependencies thus occur because coarse grains are excavated from greater depth, where ^{10}Be concentrations are lower. The highest number of negative grain size dependencies are found in catchments steeper than 25°. In these catchments, many hillslopes have likely reached the critical hillslope angle of ~25-30°, at which hillslopes cannot get any steeper and denudation rates are dominated by the frequency of landslides (Montgomery and Brandon, 2002; Ouimet et al., 2009). It is notable that the most-negative grain size dependencies occur in catchments underlain by sedimentary rocks (Table S4 and Figure S4). This may be due to lower rock mass strength of sedimentary rocks, which partly stems from the presence of bedding planes, and which may make them more susceptible to hillslope failure (e.g., Clarke and Burbank, 2011; Perras and Diederichs, 2014). Our results conform with previous studies that also found negative grain size dependencies as result of deep-seated erosion processes (Brown et al., 1995; Lukens et al., 2016; Reinhardt et al., 2007; Tofelde et al., 2018).

6.2.2 Sediment travel distance

Our results show that negative grain size dependencies are more frequent in catchments with long sediment travel distances (Figure 7b), in particular when travel distances exceed our estimates of the abrasion threshold distance, i.e., the distance after which abrasion has likely reduced a grain to half its original size. A potential explanation for this observation is that travel distance scales with elevation (Figure S6) and sediment from high elevations may have inherently higher nuclide concentrations because nuclide production rates are higher at higher elevation (Lal, 1991). Due to abrasion, these distant sources may thus be overrepresented in the finer fractions, and underrepresented in the coarser ones (Lukens et al., 2016). If true, this would mean that grain size fractions at the sample location of large catchments may be non-representative for the entire catchment. Grain size dependencies at long mean travel distances are predominantly negative for catchments with sedimentary or mixed rock types. Possibly the lower rock strength of sedimentary rocks promotes the breakdown into smaller particles and increases the grain's sensitivity to abrasion (Attal and Lavé, 2009; Sklar and Dietrich, 2001). In catchments with mixed lithologies, the provenance of distinct grain sizes from different lithologies could additionally induce non-representative grain size fractions. Such an effect would be particularly important if the different lithologies are located at different elevations (e.g. Matmon et al., 2003). If abrasion were to reduce river sediment of decimetre- or meter-scale to sand size, the shielded interior of such clasts would have lower concentrations (Carretier and Regard, 2011; Lupker et al., 2017). However, the associated travel distance would have to be considerably longer, and the initial clast must be large. For example, abrasion of an initial 25 cm sized granitic cobble over a distance of ~8 km would result in a size reduction of 10 cm in size and expose a centre with a ^{10}Be concentration that is only 8.5% lower compared to the outer layers (Balco et al., 2008; Sklar et al., 2006). The by-product of abrasion, which typically is of silt or clay size (Sklar et al., 2006), unlikely affects the measured ^{10}Be concentrations, as it is finer than the grain size classes typically analysed (Lukens et al., 2016). Finally, transient storage of fine grains in floodplains is also unlikely to account for the observed grain size dependence in ^{10}Be concentrations, because we only considered relatively small catchments, in which transient storage is likely short and insufficient to account for significant additional ^{10}Be accumulation

6.2.3 Mean Annual Precipitation

Negative grain size dependencies are predominantly found in arid (<100 mm yr^{-1}) and humid catchments (>2000 mm yr^{-1}), whereas Mediterranean and temperate catchments (100–2000 mm yr^{-1}) show no or only a weak grain size dependency. This conforms to the results from our case study in the Chilean Coastal Cordillera, which also shows a negative grain size dependency in the most-arid catchment (AZ) and no grain size trend in the temperate catchment (NA). The climatic gradient in our case study did not include a humid catchment with MAP >2000 mm yr^{-1} but negative grain size dependences in humid catchments may result from precipitation-induced landslides during extreme rain events (Chang et al., 2007; Chen et al., 2006; Lin et al., 2008). We thus think that the observed grain size dependencies in the global compilation could be related to the effect of MAP on the thickness of mixed soil layer and the scouring depth of erosion processes.

6.3 Implications

Our results and the above discussion suggest that grain size trends in ^{10}Be concentrations are best explained in the context of the presence and thickness of mixed soil layers and the scouring depth of hillslope erosion processes. In large catchments, an additional effect may emerge, resulting from abrasion and sediment provenance processes. At present, however, it is difficult to quantify the relative roles of hillslope angle, precipitation, travel distance, and lithology, because these parameters tend to be partly correlated. For example, high and steep topography is often associated with high amounts of orographic precipitation, and long travel distances are associated with large catchments (Figure S6), where the chance for multiple lithologies is higher than for smaller catchments.

In any case, the presumed role that soils and different hillslope erosion processes play for grain size-dependent ^{10}Be concentrations is likely not linearly related to variables like mean hillslope angle or mean annual precipitation. Instead, our results are consistent with the presence of thresholds. Landslides likely become important when hillslope angles exceed a critical threshold value (Burbank et al., 1996). And once precipitation is high enough to sustain vegetation and soils, diffusive processes may dominate gently-sloping and soil-mantled landscapes. Such a threshold control on the occurrence of grain size-dependent ^{10}Be concentrations may be the reason why our multivariate statistics, using a linear model, yielded mostly insignificant results (Figure 9 and Table S5). More data may allow better constraining the relative importance of these factors in the future. It additionally highlights the importance of studies on single factors, like our study on the sole effect of MAP in the Chilean Coastal Cordillera.

We evaluated the likelihood of grain size-dependent ^{10}Be concentrations and a potential bias in previously published ^{10}Be-derived catchment-average denudation rates, by comparing our findings with a recently published global compilation (Codilean et al., 2018). Out of 2537 different catchments with an area <5000 km^2, 55.7% have hillslope angles >15°, where our data first shows significant grain size effects, and 23.3% exceeded the threshold hillslope angle >25°. When considering sediment travel distances, using the relationship between catchment area and sediment travel distance that emerged from our global compilation (R^2= 0.99; Figure S6) about 61.9%, 49.8% and 29.2% of the catchments have exceeded the sediment travel distances of >2300 m, >3500 m and >7000 m, respectively. Finally, 2.8% of the catchments have MAP <100 mm yr^{-1} and 11.5% have MAP >2000 mm yr^{-1}, based on GPCC-derived MAP at the sample location. Therefore, previously published catchment-average denudation rates may more

frequently be biased as a result of steep hillslopes and long sediment travel distance and less frequently by the influence of MAP. When considering a combined effect of all controlling factors in each catchment (slope >25°, sediment travel distance >7000 m and MAP <100 or >2000 mm yr^{-1}), 48.0% of the catchments are predicted to be devoid of grain size dependencies of ^{10}Be concentrations and biased catchment-average denudation rates, whereas 52.0% might contain a bias because one or more of the controlling factors has exceeded the threshold values that emerged from our study.

7. Conclusion

In this paper, we used a field study in Chile and a global compilation of previously published data to assess in what type of catchments grain size-dependent ^{10}Be concentrations may lead to biased estimates in catchment-average denudation rates. Our results show that the influence of mean annual precipitation on grain size dependencies appears to be limited to very arid (<100 mm yr^{-1}) or humid catchments (>2000 mm yr^{-1}). Hillslope steepness (>25°) appears to exert a more important influence. We related the effect of mean annual precipitation and mean basin slope to the presence and thickness of mixed soil layers and the scouring depth of erosion processes. Furthermore, grain size-dependent ^{10}Be concentrations may occur in large catchments with long sediment travel distances (>2300 m to >7000 m, depending on lithology), where abrasion and sediment provenance may induce non-representative grain size distributions. Due to the presence of thresholds, mean annual precipitation, catchment steepness and sediment travel distance appear to be non-linearly related to grain size-dependent ^{10}Be concentrations, which complicates efforts to disentangle and quantify their relative roles. The results of our study can be used to evaluate whether catchment-average denudation rates may be biased in particular catchments.

8. Dataset availability

All supplementary tables (S1-S5) and figures (S1-S6) are available in the data supplement (van Dongen et al., in review): http://doi.org/10.5880/GFZ.3.3.2018.004 (link not active yet, temporary link provided to reviewers). These data are freely available under the Creative Commons Attribution 4.0 International (CC BY 4.0) open access license at GFZ data services. When using the data please cite this paper.

9. Sample availability

The metadata of all samples in Table 2 can be accessed via http://igsn.org/[*insert IGSN number here*].

10. Author contributions

R. van Dongen carried out fieldwork, laboratory work, and data evaluation. D. Scherler conceived the study and was the main advisor during fieldwork, data evaluation, and manuscript writing. H. Wittmann was responsible for the cosmogenic-^{10}Be laboratory training and laboratory supervision. F. von Blanckenburg and H. Wittmann were

available for extensive discussion during data evaluation. R. van Dongen prepared the manuscript with contributions from all co-authors.

11. Competing interests

The authors declare that they have no conflict of interest.

12. Acknowledgements

We acknowledge support from the German Science Foundation (DFG) priority research program SPP-1803 "EarthShape: Earth Surface Shaping by Biota" (grant SCHE 1676/4-1 to D.S.). We are grateful to the Chilean National Park Service (CONAF) for providing access to the sample locations and on-site support of our research. We also thank Dr. L. Mao, R. Carrillo and M. Koelewijn for their support during fieldwork, Dr. S. Binnie and Dr. S. Heinze from Cologne University for conducting AMS measurements, and Dr. M. Henehan for his help with statistical analysis.

13. References

Aguilar, G., Carretier, S., Regard, V., Vassallo, R., Riquelme, R. and Martinod, J.: Grain size-dependent ^{10}Be concentrations in alluvial stream sediment of the Huasco Valley, a semi-arid Andes region, Quat. Geochronol., 19, 163–172, doi:10.1016/j.quageo.2013.01.011, 2014.

Allen, P. A., Armitage, J. J., Whittaker, A. C., Michael, N. A., Roda-boluda, D. and Arcy, M. D.: Fragmentation Model of the Grain Size Mix of Sediment Supplied to Basins, J. Geol., 123, 405–427, doi:10.1086/683113, 2015.

Anderson, S. P., von Blanckenburg, F. and White, A.: Physical and Chemical Controls on the Chritical Zone, Elements, 3(5), 315–319, doi:10.2113/gselements.3.5.315, 2007.

Attal, M. and Lavé, J.: Pebble abrasion during fluvial transport: Experimental results and implications for the evolution of the sediment load along rivers, J. Geophys. Res. Earth Surf., 114(4), 1–22, doi:10.1029/2009JF001328, 2009.

Attal, M., Mudd, S. M., Hurst, M. D., Weinman, B., Yoo, K. and Naylor, M.: Impact of change in erosion rate and landscape steepness on hillslope and fluvial sediments grain size in the Feather River Basin (Sierra Nevada, California), Earth Surf. Dyn. Discuss., 2(2), 1047–1092, doi:10.5194/esurfd-2-1047-2014, 2014.

Balco, G., Stone, J. O., Lifton, N. A. and Dunai, T. J.: A complete and easily accessible means of calculating surface exposure ages or erosion rates from 10Be and 26Al measurements, Quat. Geochronol., 3(3), 174–195, doi:10.1016/j.quageo.2007.12.001, 2008.

Belmont, P., Pazzaglia, F. J. and Gosse, J. C.: Cosmogenic ^{10}Be as a tracer for hillslope and channel sediment dynamics in the Clearwater River, western Washington State, Earth Planet. Sci. Lett., 264(1–2), 123–135, doi:10.1016/j.epsl.2007.09.013, 2007.

Bierman, P. R. and Steig, E. J.: Estimating rates of denudation using cosmogenic isotope abundances in sediment, Earth Surf. Process. Landforms, 21(2), 125–139, doi:10.1002/(SICI)1096-9837(199602)21:2<125::AID-ESP511>3.0.CO;2-8, 1996.

von Blanckenburg, F.: The control mechanisms of erosion and weathering at basin scale from cosmogenic nuclides in river sediment, Earth Planet. Sci. Lett., 237(3–4), 462–479, doi:10.1016/j.epsl.2005.06.030, 2005.

von Blanckenburg, F., Hewawasam, T. and Kubik, P. W.: Cosmogenic nuclide evidence for low weathering and denudation in the wet , tropical highlands of Sri Lanka, J. Geophys. Res., 109, doi:10.1029/2003JF000049, 2004.

Brown, E. T., Stallard, R. F., Larsen, M. C., Raisbeck, G. M. and Yiou, F.: Denudation rates determined from the accumulation of in situ-produced ^{10}Be in the luquillo experimental forest, Puerto Rico, Earth Planet. Sci. Lett., 129(1–4), 193–202, doi:10.1016/0012-821X(94)00249-X, 1995.

Burbank, D. W., Leland, J., Fielding, E., Anderson, R. S., Brozovic, N., Reid, M. R. and Duncan, C.: Bedrock incision, rock uplift and threshold hillslopes in the northwestern Himalayas, Nature, 379, 505–510, doi:https://doi.org/10.1038/379505a0, 1996.

Carretier, S. and Regard, V.: Is it possible to quantify pebble abrasion and velocity in rivers using terrestrial cosmogenic nuclides?, J. Geophys. Res. Earth Surf., 116(4), 1–17, doi:10.1029/2011JF001968, 2011.

Carretier, S., Regard, V. and Soual, C.: Theoretical cosmogenic nuclide concentration in river bed load clasts: Does it depend on clast size?, Quat. Geochronol., 4(2), 108–123, doi:10.1016/j.quageo.2008.11.004, 2009.

Carretier, S., Regard, V., Vassallo, R., Aguilar, G., Martinod, J., Riquelme, R., Christophoul, F., Charrier, R., Gayer, E., Farías, M., Audin, L. and Lagane, C.: Differences in ^{10}Be concentrations between river sand, gravel and pebbles along the western side of the central Andes, Quat. Geochronol., 27(April), 33–51, doi:10.1016/j.quageo.2014.12.002, 2015.

Casagli, N., Ermini, L. and Rosati, G.: Determining grain size distribution of the material composing landslide dams in the Northern Apennines: Sampling and processing methods, Eng. Geol., 69(1–2), 83–97, doi:10.1016/S0013-7952(02)00249-1, 2003.

Chang, K. T., Chiang, S. H. and Hsu, M. L.: Modeling typhoon- and earthquake-induced landslides in a mountainous watershed using logistic regression, Geomorphology, 89(3–4), 335–347, doi:10.1016/j.geomorph.2006.12.011, 2007.

Chen, H., Dadson, S. and Chi, Y. G.: Recent rainfall-induced landslides and debris flow in northern Taiwan, Geomorphology, 77(1–2), 112–125, doi:10.1016/j.geomorph.2006.01.002, 2006.

Clapp, E. M., Bierman, P. R. and Caffee, M.: Using ^{10}Be and ^{26}Al to determine sediment generation rates and identify sediment source areas in an arid region drainage basin, Geomorphology, 45(1–2), 89–104, doi:10.1016/S0169-555X(01)00191-X, 2002.

Clarke, B. A. and Burbank, D. W.: Quantifying bedrock - fracture patterns within the shallow subsurface : Implications for rock mass strength , bedrock landslides, and erodibility, J. Geophys. Res., 116(F04009), doi:10.1029/2011JF001987, 2011.

Codilean, A. T., Munack, H., Cohen, T. J., Saktura, W. M., Gray, A. and Mudd, S. M.: OCTOPUS: An Open Cosmogenic Isotope and Luminescence Database, Earth Syst. Sci. Data Discuss., (March), 1–23, doi:10.5194/essd-2018-32, 2018.

Crosby, B. T. and Whipple, K. X.: Knickpoint initiation and distribution within fluvial networks: 236 waterfalls in the Waipaoa River, North Island, New Zealand, Geomorphology, 82(1–2), 16–38, doi:10.1016/j.geomorph.2005.08.023, 2006.

Derrieux, F., Siame, L. L., Bourlès, D. L., Chen, R. F., Braucher, R., Léanni, L., Lee, J. C., Chu, H. T. and Byrne, T. B.: How fast is the denudation of the Taiwan mountain belt? Perspectives from in situ cosmogenic ^{10}Be, J. Asian Earth Sci., 88, 230–245, doi:10.1016/j.jseaes.2014.03.012, 2014.

DiBiase, R. A. and Whipple, K. X.: The influence of erosion thresholds and runoff variability on the relationships among topography, climate, and erosion rate, J. Geophys. Res., 116(F4), F04036, doi:10.1029/2011JF002095, 2011.

Didan, K.: MOD13Q1 MODIS/Terra Vegetation Indices 16-Day L3 Global 250m SIN Grid V006 [Data set], , doi:10.5067/MODIS/MOD13Q1.006, 2015.

Dixon, J. L. and von Blanckenburg, F.: Soils as pacemakers and limiters of global silicate weathering, Comptes Rendus - Geosci., 344(11–12), 597–609, doi:10.1016/j.crte.2012.10.012, 2012.

van Dongen, R., Scherler, D., Wittmann, H. and von Blanckenburg, F.: Data supplement to: Cosmogenic ^{10}Be in river sediment: where grain size matters and why, GFZ Data Serv., doi:http://doi.org/10.5880/GFZ.3.3.2018.004, in review.

Ferguson, R., Hoey, T., Wathen, S. and Werritty, A.: Field evidence for rapid downstream fining of river gravels through selective transport, Geology, 24(2), 179–182, doi:10.1130/0091-7613(1996)024<0179:FEFRDF>2.3.CO;2, 1996.

Gabet, E. J., Reichman, O. J. and Seabloom, E. W.: The Effects of Bioturbation on Soil Processes and Sediment Transport, Annu. Rev. Earth Planet. Sci., 31(1), 249–273, doi:10.1146/annurev.earth.31.100901.141314, 2003.

Glodny, J., Graaefe Kirsten and Rosenau, M.: Mesozoic to Quaternary continental margin dynamics in South-Central Chile (36 – 42 ° S): the apatite and zircon fission track perspective, Int. J. Earth Sci., 97, 1271–1291, doi:10.1007/s00531-007-0203-1, 2008.

Gonzalez, V. S., Schmidt, A. H., Bierman, P. R. and Rood, D. H.: Spatial and temporal replicability of meteoric and in situ ^{10}Be concentrations in fluvial sediment, Earth Surf. Process. Landforms, 42(15), 2570–2584, doi:10.1002/esp.4205, 2017.

Gosse, J. C. and Phillips, F. M.: Terrestrial in situ cosmogenic nuclides:theory and application, Quat. Sci. Rev., 20, 1475–1560, doi:10.1016/S0277-3791(00)00171-2, 2001.

Granger, D., Kirchner, J. and Finkel, R.: Spatially averaged long-term erosion rates measured from in situ-produced cosmogenic nuclides in alluvial sediment, J. Geol., 104(3), 249–257, doi:10.1086/629823, 1996.

Grömping, U.: R package relaimpo: relative importance for linear regression, J. Stat. Softw., 17(1), 139–147, doi:10.1016/j.foreco.2006.08.245, 2006.

Hartmann, J. and Moosdorf, N.: The new global lithological map database GLiM: A representation of rock properties at the Earth surface, Geochemistry, Geophys. Geosystems, 13(12), 1–37, doi:10.1029/2012GC004370, 2012.

Heimsath, A. M., Fink, D. and Hancock, G. R.: The " humped " soil production function : eroding Arnhem Land , Australia, Earth Surf. Process. Landforms, 1684, 1674–1684, doi:10.1002/esp.1859, 2009.

Hoey, T. B. and Ferguson, R.: Numerical simulation of downstream fining by selective transport in gravel bed rivers: Model development and illustration, Water Resour., 30(7), 2251–2260, doi:https://doi.org/10.1029/94WR00556, 1994.

Hovius, N., Stark, C. A. and Allen, P. A.: Sediment flux from a mountain belt derived by landsliding mapping, Geology, 25(3), 231–234, doi:10.1130/0091-7613(1997)025<0231:SFFAMB>2.3.CO;2, 1997.

Jarvis, A., Reuter, H. I., Nelson, A. and Guevara, E.: Hole-filled SRTM for the globe Version 4, available from the CGIAR-CSI SRTM 90m Database, [online] Available from: http://srtm.csi.cgiar.org, 2008.

Kodama, Y.: Previous Studies of Abrasion on Downstream Fining Purpose of This Study, J. Sediment. Res., A64(1), 68–75, 1994.

Kodoma, Y.: Experimental Study of Abrasion and Its Role in Producing Downstream Fining in Gravel-Bed Rivers, J. Sediment. Res., 64A(1), 76–85, 1994.

Kohl, C. P. and Nishiizumi, K.: Chemical isolation of quartz for measurement of in-situ -produced cosmogenic nuclides, Geochim. Cosmochim. Acta, 56(9), 3583–3587, doi:10.1016/0016-7037(92)90401-4, 1992.

Lal, D.: Cosmic ray labeling of erosion surfaces : in situ nuclide production rates and erosion models, Earth Planet. Sci. Lett., 104, 424–439, 1991.

Lasaga, A. C., Soler, J. M., Burch, T. E. and Nagy, K. L.: Chemical weathering rate laws and global geochemical cycles, Geochim. Cosmochim. Acta, 58(10), 2361–2386, 1994.

Lebedeva, M. I. and Brantley, S. L.: Weathering and erosion of fractured bedrock systems, Earth Surf. Process. Landforms, 42(13), 2090–2108, doi:10.1002/esp.4177, 2017.

Lewin, J. and Brewer, P. A.: Laboratory Simulation of Clast Abrasion, Earth Surf. Process. Landforms, 27, 145–164, doi:10.1177/0022034509333968, 2002.

Lin, G. W., Chen, H., Chen, Y. H. and Horng, M. J.: Influence of typhoons and earthquakes on rainfall-induced landslides and suspended sediments discharge, Eng. Geol., 97(1–2), 32–41, doi:10.1016/j.enggeo.2007.12.001, 2008.

Lukens, C. E., Riebe, C. S., Sklar, L. S. and Shuster, D. L.: Grain size bias in cosmogenic nuclide studies of stream sediment in steep terrain, J. Geophys. Res. Earth Surf., 121, 978–999, doi:10.1002/2016JF003859.Received, 2016.

Lupker, M., Lavé, J., France-Lanord, C., Christl, M., Bourlès, D. L., Carcaillet, J., Maden, C., Wieler, R., Rahman, M., Bezbaruah, D. and Xiaohan, L.: ^{10}Be systematics in the Tsangpo-Brahmaputra catchment: the cosmogenic nuclide legacy of the eastern Himalayan syntaxis, Earth Surf. Dyn., 9(2), 429–449, 2017.

Maher, K.: The dependence of chemical weathering rates on fluid residence time, Earth Planet. Sci. Lett., 294(1–2), 101–110, doi:10.1016/j.epsl.2010.03.010, 2010.

Mather, A. E., Hartley, A. J. and Griffiths, J. S.: The giant coastal landslides of Northern Chile: Tectonic and climate interactions on a classic convergent plate margin, Earth Planet. Sci. Lett., 388, 249–256, doi:10.1016/j.epsl.2013.10.019, 2014.

Matmon, A., Bierman, P. R., Larsen, J., Southworth, S., Pavich, M., Finkel, R. and Caffee, M.: Erosion of an ancient mountain range, the Great Smoky Mountains, North Carolina and Tennessee, Am. J. Sci., 303(9), 817–855, doi:10.2475/ajs.303.9.817, 2003.

Melnick, D.: Rise of the central Andean coast by earthquakes straddling the Moho, Nat. Geosci., (March), 1–8, doi:10.1038/ngeo2683, 2016.

Melnick, D., Bookhagen, B., Strecker, M. R. and Echtler, H. P.: Segmentation of megathrust rupture zones from fore-arc deformation patterns over hundreds to millions of years, Arauco peninsula, Chile, J. Geophys. Res. Solid Earth, 114(1), 1–23, doi:10.1029/2008JB005788, 2009.

Meyer-Christoffer, A., Becker, A., Finger, P., Rudolf, B., Schneider, U. and Ziese, M.: GPCC Climatology Version 2015 at 0.25°: Monthly Land-Surface Precipitation Climatology for Every Month and the Total Year from Rain-Gauges built on GTS-based and Historic Data., 2015.

Montgomery, D. R. and Brandon, M. T.: Topographic controls on erosion rates in tectonically active mountain ranges, Earth Planet. Sci. Lett., 201(3–4), 481–489, doi:10.1016/S0012-821X(02)00725-2, 2002.

Neilson, T. B., Schmidt, A. H., Bierman, P. R., Rood, D. H. and Sosa Gonzalez, V.: Efficacy of in situ and meteoric ^{10}Be mixing in fluvial sediment collected from small catchments in China, Chem. Geol., 471(September), 119–130, doi:10.1016/j.chemgeo.2017.09.024, 2017.

Oberlander, T. M.: Morphogenesis of Granitic Boulder Slopes in the Mojave Desert, California, J. Geol., 80(1), 1–20, 1972.

Oeser, R. A., Stroncik, N., Moskwa, L., Bernhard, N., Schaller, M., Canessa, R., Brink, L. Van Den, Köster, M., Brucker, E., Stock, S., Pablo, J., Godoy, R., Javier, F., Oses, R., Osses, P., Paulino, L., Seguel, O., Bader, M. Y., Boy, J., Dippold, M. A., Ehlers, T. A., Kühn, P., Kuzyakov, Y., Leinweber, P., Scholten, T., Spielvogel, S., Spohn, M., Übernickel, K., Tielbörger, K., Wagner, D. and Blanckenburg, F. Von: Chemistry and microbiology of the Critical Zone along a steep climate and vegetation gradient in the Chilean Coastal Cordillera, Catena, 170(April), 183–203, doi:10.1016/j.catena.2018.06.002, 2018.

Ouimet, W. B., Whipple, K. X. and Granger, D. E.: Beyond threshold hillslopes: Channel adjustment to base-level fall in tectonically active mountain ranges, Geology, 37(7), 579–582, doi:10.1130/G30013A.1, 2009.

Palumbo, L., Hetzel, R., Tao, M. and Li, X.: Catchment-wide denudation rates at the margin of NE Tibet from in situ-produced cosmogenic ^{10}Be, Terra Nov., 23(1), 42–48, doi:10.1111/j.1365-3121.2010.00982.x, 2011.

Perras, M. A. and Diederichs, M. S.: A Review of the Tensile Strength of Rock: Concepts and Testing, Geotech. Geol. Eng., 32(2), 525–546, doi:10.1007/s10706-014-9732-0, 2014.

Phillips, F. M., Argento, D. C., Balco, G., Caffee, M. W., Clem, J., Dunai, T. J., Finkel, R., Goehring, B., Gosse, J. C., Hudson, A. M., Jull, A. J. T., Kelly, M. A., Kurz, M., Lal, D., Lifton, N., Marrero, S. M., Nishiizumi, K., Reedy, R. C., Schaefer, J., Stone, J. O. H., Swanson, T. and Zreda, M. G.: The CRONUS-Earth Project: A synthesis, Quat. Geochronol., 31, 119–154, doi:10.1016/j.quageo.2015.09.006, 2016.

Pinto, L., Hérail, G., Sepúlveda, S. A. and Krop, P.: A Neogene giant landslide in Tarapacá, northern Chile: A signal of instability of the westernmost Altiplano and palaeoseismicity effects, Geomorphology, 102(3–4), 532–541, doi:10.1016/j.geomorph.2008.05.044, 2008.

Portenga, E. W. and Bierman, P. R.: Understanding earth's eroding surface with ^{10}Be, GSA Today, 21(8), 4–10, doi:10.1130/G111A.1, 2011.

Puchol, N., Lavé, J., Lupker, M., Blard, P. H., Gallo, F. and France-Lanord, C.: Grain-size dependent concentration of cosmogenic ^{10}Be and erosion dynamics in a landslide-dominated Himalayan watershed, Geomorphology, 224(November), 55–68, doi:10.1016/j.geomorph.2014.06.019, 2014.

Reinhardt, L. J., Hoey, T. B., Barrows, T. T., Dempster, T. J., Bishop, P. and Fifield, L. K.: Interpreting erosion rates from cosmogenic radionuclide concentrations measured in rapidly eroding terrain, Earth Surf. Process. Landforms, 32, 390–406, doi:10.1002/esp.1415, 2007.

Riebe, C. S., Kirchner, J. W. and Finkel, R. C.: Long-term rates of chemical weathering and physical erosion from cosmogenic nuclides and geochemical mass balance, Geochim. Cosmochim. Acta, 67(22), 4411–4427, doi:10.1016/S0016-7037(03)00382-X, 2003.

Roda-Boluda, D. C., D'Arcy, M., McDonald, J. and Whittaker, A. C.: Lithological controls on hillslope sediment supply: insights from landslide activity and grain size distributions, Earth Surf. Process. Landforms, 43(5), 956–977, doi:10.1002/esp.4281, 2018.

Roering, J. J., Kirchner, J. W. and Dietrich, W. E.: Evidence for nonlinear, diffusive sediment transport on hillslopes and implications for landscape morphology, Water Resour. Res., 35(3), 853–870, doi:10.1029/1998WR900090, 1999.

Ruxton, B. P. and Berry, L.: Weathering of granite and associated erosional features in Hong Kong, Bull. Geol. Soc. Am., 68(10), 1263–1292, doi:10.1130/0016-7606(1957)68[1263:WOGAAE]2.0.CO;2, 1957.

Schaller, M., Ehlers, T. A., Lang, K. A. H., Schmid, M. and Fuentes-Espoz, J. P.: Addressing the contribution of climate and vegetation cover on hillslope denudation, Chilean Coastal Cordillera (26°–38°S), Earth Planet. Sci. Lett., 489, 111–122, doi:10.1016/j.epsl.2018.02.026, 2018.

Scherler, D., Lamb, M. P., Rhodes, E. J. and Avouac, J. P.: Climate-change versus landslide origin of fill terraces in a rapidly eroding bedrock landscape: San Gabriel River, California, Bull. Geol. Soc. Am., 128(7), 1228–1248, doi:10.1130/B31356.1, 2016.

Schildgen, T. F., Robinson, R. A. J., Savi, S., Phillips, W. M., Spencer, J. Q. G., Bookhagen, B., Scherler, D., Tofelde, S., Alonso, R. N., Kubik, P. W., Binnie, S. A. and Strecker, M. R.: Landscape response to late Pleistocene climate change in NW Argentina: Sediment flux modulated by basin geometry and connectivity, J. Geophys. Res. Earth Surf., 121, 392–414, doi:10.1002/2015JF003607, 2016.

Sklar, L. S. and Dietrich, W. E.: Sediment and rock strength controls on river incision into bedrock, Geology, 29(12), 1087–1090, doi:https://doi.org/10.1130/0091-7613(2001)029<1087:SARSCO>2.0.CO;2, 2001.

Sklar, L. S. and Dietrich, W. E.: Implications of the Saltation-Abrasion Bedrock Incision Model for Steady-State River Longitudinal Profile Relief and Concavity, Earth Surf. Process. Landforms, 33(7), 1129–1151, doi:10.1002/esp, 2008.

Sklar, L. S., Dietrich, W. E., Foufoula-Georgiou, E., Lashermes, B. and Bellugi, D.: Do gravel bed river size distributions record channel network structure?, Water Resour. Res., 42(SUPPL.), 1–22, doi:10.1029/2006WR005035, 2006.

Sklar, L. S., Riebe, C. S., Marshall, J. A., Genetti, J., Leclere, S., Lukens, C. L. and Merces, V.: The problem of predicting the size distribution of sediment supplied by hillslopes to rivers, Geomorphology, 277, 31–49, doi:10.1016/j.geomorph.2016.05.005, 2017.

Stock, G. M., Frankel, K. L., Ehlers, T. a., Schaller, M., Briggs, S. M. and Finkel, R. C.: Spatial and temporal variations in denudation of the Wasatch Mountains, Utah, USA, Lithosphere, 1, 34–40, doi:10.1130/L15.1, 2009.

Stone, J. O.: Air pressure and cosmogenic isotope production, J. Geophys. Res., 105(1), 753–759, doi:10.1029/2000JB900181, 2000.

Sullivan, C. L.: ^{10}Be Erosion Rates and Landscape Evolution of the Blue Ridge Escarpment, Southern Appalachian Mountains, 2007.

Tofelde, S., Duesing, W., Schildgen, T. F., Wickert, A. D., Wittmann, H., Alonso, R. N. and Strecker, M.: Effects of deep-seated versus shallow hillslope processes on cosmogenic^{10}Be concentrations in fluvial sand and gravel, Earth Surf. Process. Landforms, doi:10.1002/esp.4471, 2018.

West, A. J., Hetzel, R., Li, G., Jin, Z., Zhang, F., Hilton, R. G. and Densmore, A. L.: Dilution of ^{10} Be in detrital quartz by earthquake-induced landslides : Implications for determining denudation rates and potential to provide insights into landslide sediment dynamics, Earth Planet. Sci. Lett., 396, 143–153, doi:10.1016/j.epsl.2014.03.058, 2014.

Willenbring, J. K., Gasparini, N. M., Crosby, B. T. and Brocard, G.: What does a mean mean? The temporal evolution of detrital cosmogenic denudation rates in a transient landscape, Geology, 41(12), 1215–1218, doi:10.1130/G34746.1, 2013.

Wolman, M. G.: A method of sampling coarse river-bed material, Trans. Am. Geophys. Union, 35(6), 951–956, doi:https://doi.org/10.1029/TR035i006p00951, 1954.

Earth Surf. Dynam. Discuss., https://doi.org/10.5194/esurf-2018-83
Manuscript under review for journal Earth Surf. Dynam.
Discussion started: 3 December 2018

Tables

Table 1: Sample location coordinates and catchment attributes of the research areas located in the Chilean Coastal Cordillera.

Catchment	Climate zone	Latitude (°N)	Longitude (°E)	MAP[a] (mm yr^{-1})	Area (km^2)	Mean elevation (m)	Mean slope[b] (°)	Mean channel steepness[c] $m^{0.9}$
Pan de Azúcar (AZ)	Arid	-26.112	-70.551	13	0.04	339	8.2	7.1
Santa Gracia (SG)	Semi-arid	-29.760	-71.168	88	0.88	773	17.2	32.2
La Campana (LC)	Mediterreanean	-32.954	-71.069	358	7.41	1323	23.1	88.8
Nahuelbuta (NA)	Temperate	-37.808	-73.014	1213	5.79	1308	8.9	20.5

[a] Mean annual precipitation (MAP) is derived from the GPCC dataset (Meyer-Christoffer et al., 2015).

[b] Total mean basin slope calculated with a 30m DEM.

[c] Normalized channel steepness index.

Earth Surf. Dynam. Discuss., https://doi.org/10.5194/esurf-2018-83
Manuscript under review for journal Earth Surf. Dynam.
Discussion started: 3 December 2018

690 **Table 2: IGSN number, sample mass, $^{10}Be/^{9}Be$ ratio (±1σ), ^{10}Be concentrations (±2σ) and denudation rates (±2σ) of all analysed samples.**

Catchment	Grain size (mm)	IGSN	Quartz mass (g)	^{9}Be Carrier mass (mg)	$^{10}Be/^{9}Be$ ratio ± 1σ x 10^{-14}	^{10}Be concentration ± 2σ (x 10^{5} atoms g^{-1})	Denudation rate ± 2σ [b] (mm kyr^{-1})
Pan de Azúcar (AZ)	0.5-1	GFRD10010	9.9	0.153	43.0 ± 1.5	4.48 ± 0.33	6.04 ± 0.69
	1-2	GFRD10011	17.9	0.153	79.9 ± 2.8	4.60 ± 0.34	5.86 ± 0.67
	2-4	GFRD10012	18.7	0.154	78.6 ± 5.8	4.36 ± 0.32	6.21 ± 0.72
	4-8	GFRD10013	18.2	0.153	65.3 ± 3.6	3.69 ± 0.42	7.5 ± 1.1
	8-16	GFRD10014	18.1	0.154	55.2 ± 2.1	3.14 ± 0.24	8.9 ± 1.0
	16-32	GFRD10015	15.0	0.153	40.8 ± 1.5	2.80 ± 0.21	10.2 ± 1.1
	32-64	GFRD10016	18.7	0.153	57.6 ± 2.0	3.16 ± 0.22	8.9 ± 1.0
	Mean	-	-		-	3.75 ± 0.24	7.66 ± 0.69
Santa Gracia (SG)	0.5-1	GFRD1000Q	18.7	0.154	85.4 ± 2.9	4.71 ± 0.33	8.26 ± 0.91
	1-2	GFRD1000R	14.1	0.153	55.1 ± 2.3	4.02 ± 0.34	9.8 ± 1.2
	2-4	GFRD1000S	13.8	0.153	49.0 ± 2.1	3.62 ± 0.32	11.0 ± 1.4
	4-8	GFRD1000T	13.8	0.153	50.3 ± 2.4	3.76 ± 0.37	10.5 ± 1.4
	8-16	GFRD1000U	20.0	0.154	82.5 ± 2.7	4.25 ± 0.29	9.3 ± 1.0
	16-32	GFRD1000V	19.3	0.154	97.0 ± 3.2	5.17 ± 0.35	7.48 ± 0.82
	32-64	GFRD1000W	19.5	0.154	90.9 ± 3.0	4.79 ± 0.33	8.12 ± 0.89
	Mean	-	-		-	4.33 ± 0.26	9.21 ± 0.84
La Campana (LC)	0.5-1	GFRD1000C	19.4	0.154	4.98 ± 0.28	0.264 ± 0.030	257 ± 35
	1-2	GFRD1000D	20.0	0.154	3.44 ± 0.20	0.177 ± 0.021	384 ± 55
	2-4	GFRD1000E	17.0	0.154	6.05 ± 0.30	0.366 ± 0.037	185 ± 24
	4-8	GFRD1000F	16.9	0.154	5.70 ± 0.32	0.348 ± 0.039	194 ± 27
	8-16	GFRD1000G	19.5	0.154	12.29 ± 0.54	0.648 ± 0.059	104 ± 12
	16-32	GFRD1000H	20.0	0.154	9.69 ± 0.44	0.498 ± 0.047	135 ± 17
	32-64	GFRD1000J	16.5	0.154	9.43 ± 0.43	0.588 ± 0.055	144 ± 14
	Mean	-	-		-	0.413 ± 0.033	200 ± 22
Nahuelbuta (NA)	0.5-1	GFRD10002	19.8	0.154	51.4 ± 1.8	2.67 ± 0.19	26.0 ± 2.8
	1-2	GFRD10003	18.7	0.153	49.5 ± 2.4	2.72 ± 0.27	25.6 ± 3.3
	2-4	GFRD10004	18.7	0.153	51.8 ± 1.9	2.84 ± 0.22	24.5 ± 2.8
	4-8	GFRD10005	19.2	0.154	49.7 ± 1.8	2.67 ± 0.20	26.1 ± 2.9
	8-16	GFRD10006	20.0	0.153	56.6 ± 1.9	2.90 ± 0.21	23.9 ± 2.6
	16-32	GFRD10007	19.6	0.154	43.5 ± 1.6	2.29 ± 0.18	30.6 ± 3.4
	32-64	GFRD10008	19.6	0.153	33.5 ± 1.3	1.76 ± 0.14	40.2 ± 4.5
	Mean	-	-		-	2.55 ± 0.16	27.4 ± 2.4

Earth Surf. Dynam. Discuss., https://doi.org/10.5194/esurf-2018-83
Manuscript under review for journal Earth Surf. Dynam.
Discussion started: 3 December 2018

14. Figure captions

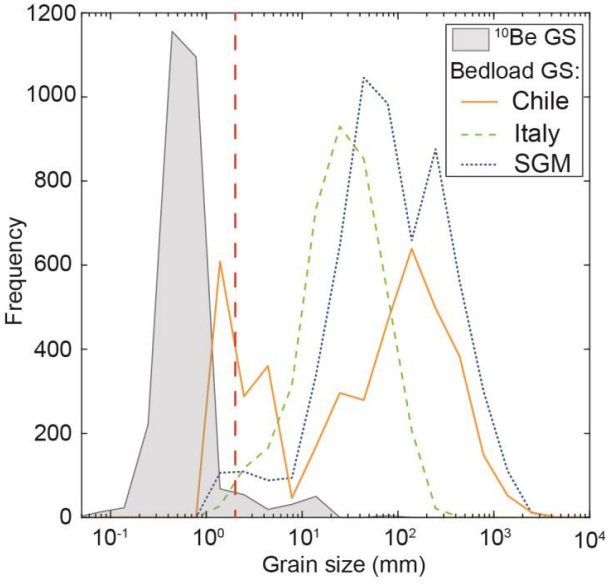

Figure 1: Grain size distributions of bedload sediment and global ^{10}Be samples. The grain sizes used for global ^{10}Be-studies (^{10}Be GS, n=2735) are derived from the OCTOPUS dataset (Codilean et al., 2018). Bedload sediment grain size distributions, measured by pebble counts, stem from representative bedrock rivers in the Chilean Coastal Cordillera (Chile, n=4246) (this study), Southern Italy and Sicily (Italy, n=3900) (Allen et al., 2015; Roda-Boluda et al., 2018) and the San Gabriel Mountains (SGM, n=5930) (DiBiase and Whipple, 2011; Scherler et al., 2016). Wolman pebble count fractions classified as <2 mm are shown as 1 mm in the figure (left of red 2 mm line).

Earth Surf. Dynam. Discuss., https://doi.org/10.5194/esurf-2018-83
Manuscript under review for journal Earth Surf. Dynam.
Discussion started: 3 December 2018

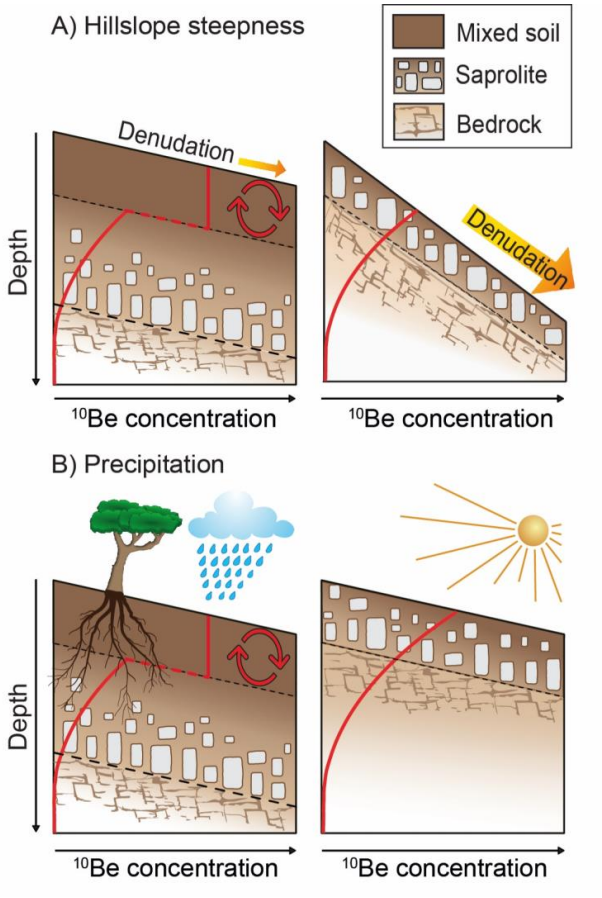

Figure 2: The effect of hillslope steepness and precipitation on the depth of the mixed soil layer and ^{10}Be concentrations as a function of depth. (A) Hillslope steepness and denudation rates control the thickness of the soil-mantle by the removal of material from the top. A thick soil-mantle likely develops in gently sloping and slowly eroding landscapes, whereas high denudation rates in steep landscapes prohibit the development of a thick soil-mantle. (B) Precipitation provides water for chemical weathering. Humid landscapes likely develop a thick soil-mantle, which may be absent in arid landscapes. Bioturbation in landscapes with thick soil-mantles results in a well-mixed soil layer with a constant ^{10}Be concentration, which, in isotopic steady state, is equal to the surface concentration. In landscapes where a mixed soil layer is absent, ^{10}Be concentrations decrease exponentially with depth.

Earth Surf. Dynam. Discuss., https://doi.org/10.5194/esurf-2018-83
Manuscript under review for journal Earth Surf. Dynam.
Discussion started: 3 December 2018

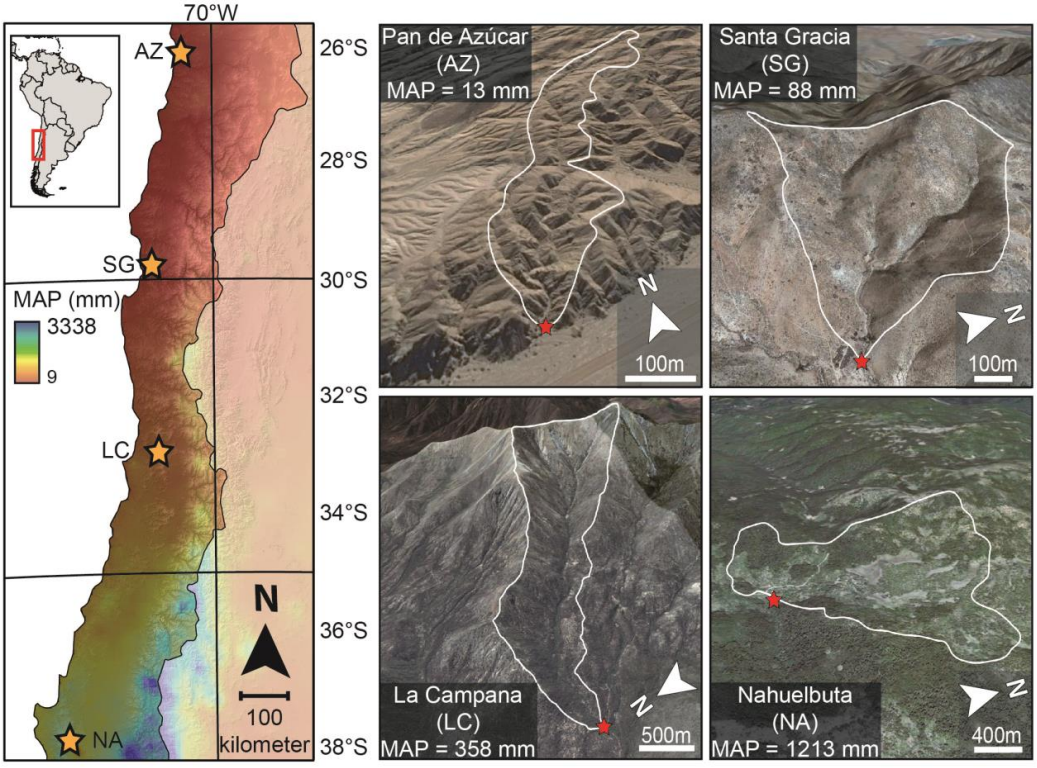

715 **Figure 3: Research areas located on a climate gradient in the Chilean Coastal Cordillera. On the left, the catchment locations (stars) on a Mean Annual Precipitation (MAP) map from Climate Hazards Group InfraRed Precipitation (CHIRPS), underlain by a SRTM DEM-derived hillshade map. On the right, Google Earth images showing the sample locations (red stars) and catchment outlines (white).**

Earth Surf. Dynam. Discuss., https://doi.org/10.5194/esurf-2018-83
Manuscript under review for journal Earth Surf. Dynam.
Discussion started: 3 December 2018

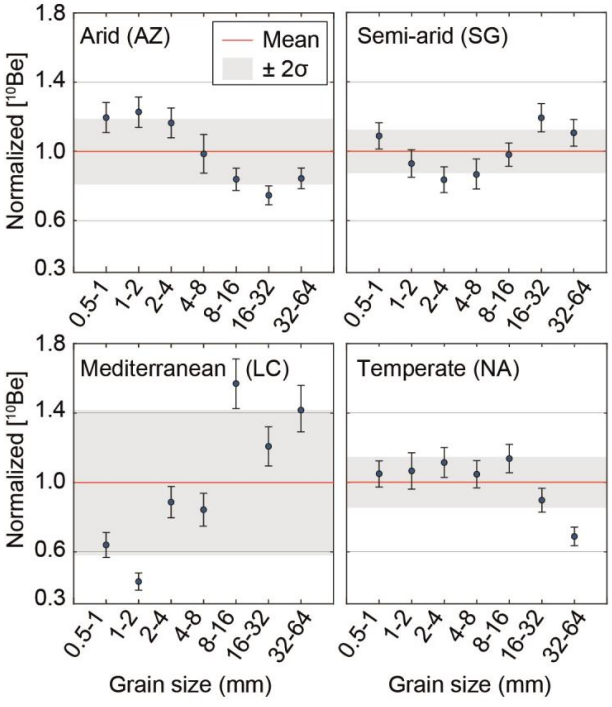

720 **Figure 4: ^{10}Be concentrations (±2σ) measured in 7 different grain size classes. The ^{10}Be concentrations are normalized to the arithmetic mean of all grain size fractions within a catchment. The red line indicates the normalized mean, grey shades represent the 2σ-deviation of individual grain size classes from the mean (AZ= ~18%, SG= ~12%, LC= ~40%, NA= ~14%).**

725

730

Earth Surf. Dynam. Discuss., https://doi.org/10.5194/esurf-2018-83
Manuscript under review for journal Earth Surf. Dynam.
Discussion started: 3 December 2018

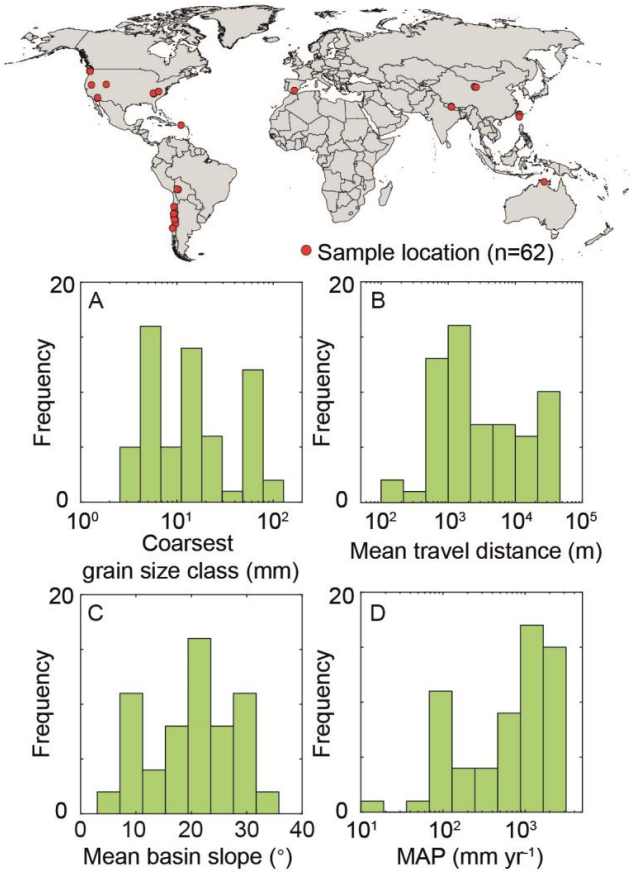

735

Figure 5: Sample locations and catchment attributes of all catchments in the global compilation (n=62). (A) Coarsest grain size classes measured in each study (the smallest grain size was always a sand fraction (<2 mm)). (B) Mean travel distance of sediment, calculated as the arithmetic mean of each grid cell's travel distance towards the catchment outlet. (C) Mean basin slope of each catchment, calculated as the arithmetic mean of the hillslope
740 **angles at each grid cell. (D) Mean annual precipitation (MAP) in each catchment, derived from the Global Precipitation Climatology Centre (GPCC) dataset.**

Earth Surf. Dynam. Discuss., https://doi.org/10.5194/esurf-2018-83
Manuscript under review for journal Earth Surf. Dynam.
Discussion started: 3 December 2018

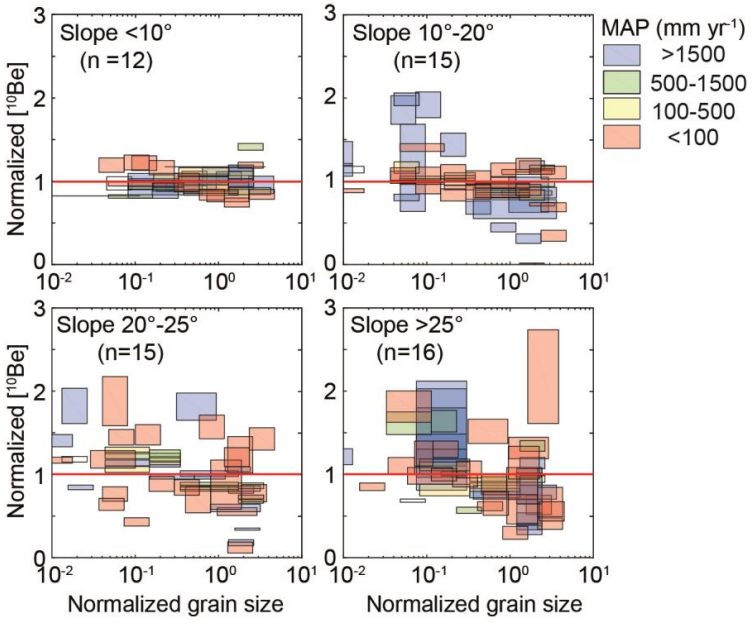

Figure 6: Global compilation results categorized into mean basin slope classes and colour-coded with mean annual precipitation (MAP). ^{10}Be concentrations (±2σ) and grain size ranges are normalized by the arithmetic mean of all samples from the same catchment.

Earth Surf. Dynam. Discuss., https://doi.org/10.5194/esurf-2018-83
Manuscript under review for journal Earth Surf. Dynam.
Discussion started: 3 December 2018

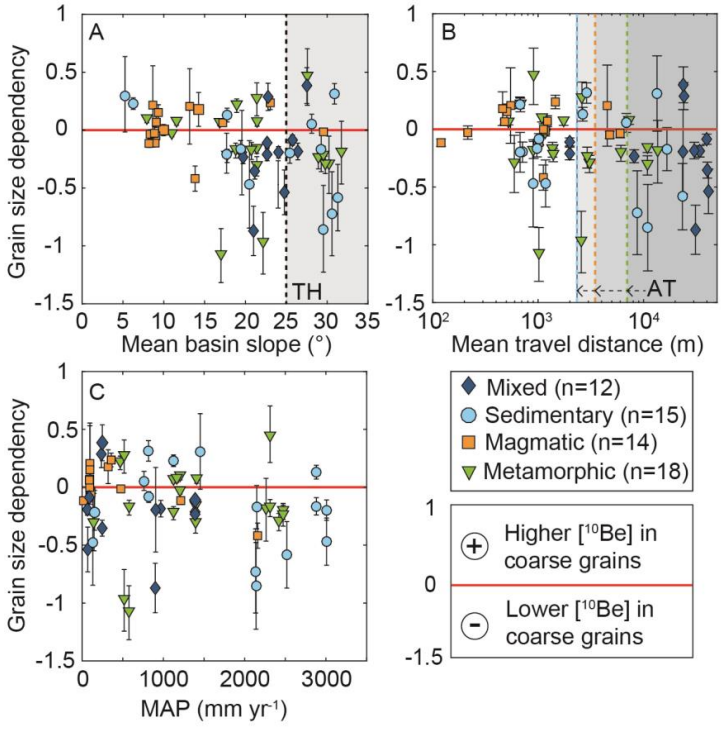

Figure 7: Grain size dependencies of all catchments in the global compilation (n=62), as a function of (A) mean basin slope, (B) mean travel distance and (C) mean annual precipitation (MAP). Grain size dependencies represent slope of a linear fit through normalized ^{10}Be concentrations and normalized grain sizes from a catchment. Coloured symbols depict lithological classes. Shaded areas represent exceeded threshold hillslopes (TH; figure A) and lithology-dependent abrasion thresholds (AT; figure B). Global compilation data is presented in Table S3, statistics and figures of individual lithologies are presented in Table S4 and Figure S4 of the data supplement.

Earth Surf. Dynam. Discuss., https://doi.org/10.5194/esurf-2018-83
Manuscript under review for journal Earth Surf. Dynam.
Discussion started: 3 December 2018

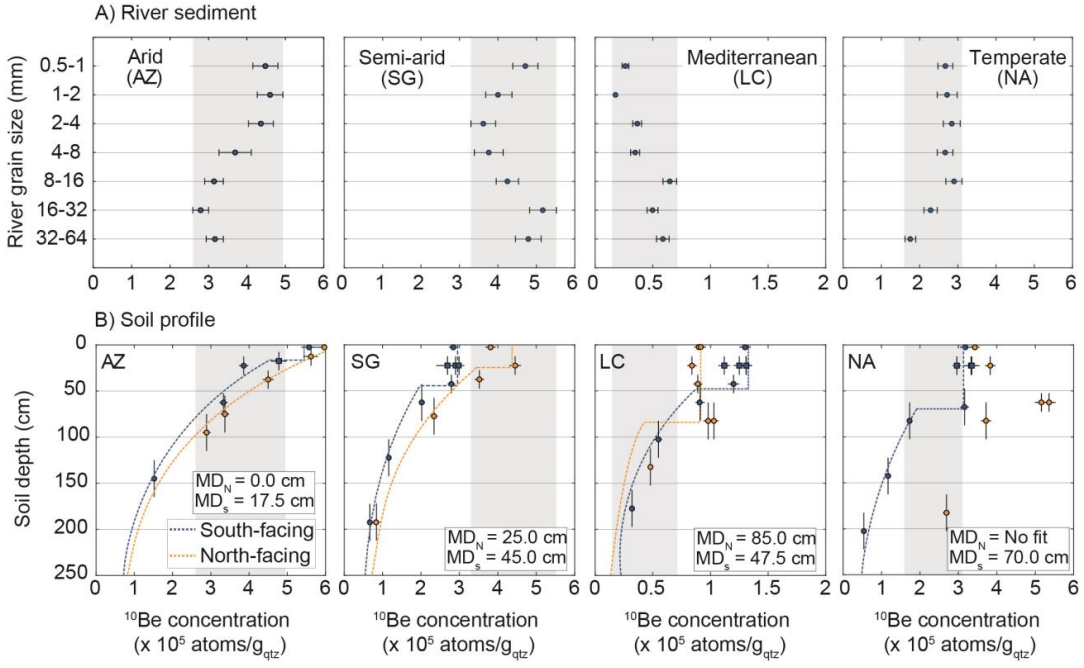

Figure 8: Comparison of ^{10}Be concentrations measured in (A) river sediment, and (B) North and South-facing soil profiles (Schaller et al., 2018), from the same catchments in the Chilean Coastal Cordillera. MD_N and MD_S are the soil mixing depths of the North and South-facing hillslopes, respectively. Note the reduced x-axis range of the Mediterranean catchment (LC). Shaded areas show range of ^{10}Be concentrations in river sediment for comparison with soil profiles.

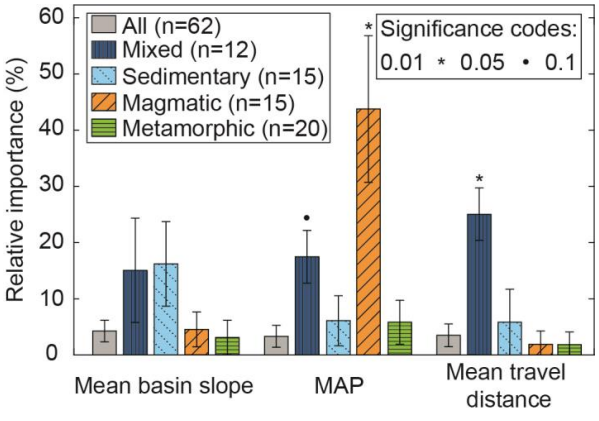

Figure 9: Relative importance of each environmental factor to the model R^2 value. Results given for all lithologies combine, and differentiated by lithology. Relative importance results are presented in Table S5.